A STUDY OF MIXING AND HEAT TRANSFER IN COMPLEX CONFIGURATIONS USING ADVANCED RANS-BASED MODELS

Alexander Yun
Department of Energy and Power Plan Technology
Technical University Darmstadt
Petersenstr. 30, 64287, Germany
yun_alexander@yahoo.de

Amsini Sadiki
Department of Energy and Power Plan Technology
Technical University Darmstadt
Petersenstr. 30, 64287, Germany
sadiki@ekt.tu-darmstadt.de

Johannes Janicka
Department of Energy and Power Plan Technology
Technical University Darmstadt
Petersenstr. 30, 64287, Germany
janicka@ekt.tu-darmstadt.de

ABSTRACT

Many turbulent flow processes of engineering importance exhibit highly complex interacting phenomena, such as mixing, heat and mass transfer, chemical reaction, etc. In curved ducts of relevance in heat exchangers, cooling passages of gas turbines and automobile engines, turbulent flow and heat transfer give rise to the existence of so-called "camel back" shapes in the streamwise mean velocity and temperature distribution of the curvature. In swirled combustion flows, turbulent flow and mixing are dominated by an extremely 3-D complex behavior of great interest for many combustion engines purposes. Both cases are complex configurations and challenging for turbulence models. In this paper the ability of advanced explicit algebraic formulation to capture such flow and mixing properties using economical costs required for engineering design purposes is successfully demonstrated.

INTRODUCTION

For many industrial and engineering purposes statistical modeling will continue to be the main approach to representing the effects of turbulent processes in CFD for technical flows regardless of recent progress in Large Eddy Simulation (LES) and novel development of statistical closures at a level higher than the first order (Leschziner, 2003). The computer resources needed and the rising trends in reducing the cost of ownership and in shortening the time to design, development and product commercialization will compel this practical way at least for several decades, especially in relation to flows that are strongly affected by viscous near-wall processes (Pope, 2001). The most of confined flows belong to this flow class. In order to simplify and adjust advanced low order models for a common use in industrial CFD some improvements at the eddy-viscosity/diffusivity level have been recorded in recent years leading to a whole category of non-linear eddy-viscosity/diffusivity based models on the one hand (Craft et al. 1996). The main challenge posed by these models is the large number of model coefficients they involve, and hence the strong sensitivity of their performance to coefficient calibration. On other hand, various and complex algebraic formulations emerge from the inversion of implicit algebraic forms of the Reynolds stress/Scalar flux vector transport equations to yield explicit forms (Wikström et al. 2000, Sadiki et al. 2003). This model class does not suffer from the calibration weakness and represent a compromise between the first class mentioned and the parent transport equations. However, in describing flows relative to non-inertial frames or in flows where local rotation rate effects of the flows are not fixed, the assumptions used to gain the appropriate implicit forms are ambiguous and mainly physically inconsistent (Gatski et al., 2004, Sadiki et al. 2003). Etemad et al. (2003) applied different non-linear models to simulate the U-bend duct flow and mixing, but fail in capturing the "camel back" shapes. Although Suga (2002) used the differential Reynolds stress tensor/scalar flux transport equations models for numerical computations of the U-bend duct, only advanced formulations could do a good, but costly job. Furthermore, no detailed discussion about the secondary motions and their impact was presented. With regard to combustor flows Jakirlic et al. (2004) used models of second order level for flow and mixing fields, and carried out 2-D simulations of swirled combustor flows. From the results it appeared that only advanced models are able to predict satisfactorily some properties while other features remain out of scope.

The question is now how to use these advanced considerations in cost-saving explicit algebraic formulations

for the calculations of complex configurations. In this work, the explicit algebraic Reynolds stress model (EARSM) of Sjögren and Johansson (2000) is extended in a consistent way by including nonlinear pressure strain rate, anisotropy dissipation and curvature correction terms. In case of curved duct a special Low-Re variant of this improved EARSM is applied. To simulate mixing and heat transfer processes a thermodynamically consistent extension of the explicit algebraic scalar flux model (EASFM) by Wikström et al. (2000) is applied following Sadiki et al. (2003).

GOVERNING EQUATIONS

The turbulent mean flow of a viscous, incompressible fluid is governed by the Reynolds-averaged continuity and Navier-Stokes equations

$$\frac{\partial \bar{u}_i}{\partial x_i} = 0\,, \tag{1}$$

$$\frac{\partial \bar{u}_i}{\partial t} + \frac{\partial \bar{u}_i \bar{u}_j}{\partial x_j} = -\frac{1}{\bar{\rho}}\frac{\partial \bar{p}}{\partial x_i} - \frac{\partial}{\partial x_j}\left(\nu \frac{\partial \bar{u}_i}{\partial x_j} + \tau_{ij}\right) + g_i\,, \tag{2}$$

where $\tau_{ij} = \overline{u_i' u_j'}$ is the unclosed Reynolds stress tensor and g_i is the gravitation force. The scalar field is described by a scalar equation of the form:

$$\frac{\partial \bar{\phi}}{\partial t} + \bar{u}_j \frac{\partial \bar{\phi}}{\partial x_j} = \frac{\partial}{\partial x_j}\left(D \frac{\partial \bar{\phi}}{\partial x_j} - Q_j\right) + \frac{1}{\bar{\rho}}\bar{S}\,, \tag{3}$$

where $Q_j = \overline{\phi' u_j'}$ is the unclosed turbulent scalar flux and $\bar{S}$ the source term (e.g. chemical reaction). The latter is not considered here. The formulations of closure relations for the Reynolds stress tensor τ_{ij} and the turbulent flux vector Q_j are based on explicit algebraic methodology.

Focused on the anisotropy stress tensor $a_{ij} = \overline{u_i' u_j'}/k - 2/3\delta_{ij}$ and the turbulent flux vector Q_j, the modeled expressions derived from the parent transport equations from which the transport of Reynolds stress tensor and scalar flux vector have to be removed in keeping the production term.

Assuming weak equilibrium in the parent transport equations the following expressions

$$\left(A_3 + A_4\frac{P}{\varepsilon}\right)a_{ij} = -A_1 S_{ij} + \left(a_{ik}\Omega_{kj} - \Omega_{ik}a_{kj}\right) - A_2\left(a_{ik}S_{kj} + S_{ik}a_{kj} - \frac{2}{3}\delta_{ij}a_{ik}S_{ki}\right), \tag{4}$$

$$P_{\phi j} - \varepsilon_{\phi j} = -\left(c_{\phi 1} + \frac{1}{2}\frac{k}{\varepsilon k_\phi}\overline{u_k'\phi'}\frac{\partial \phi}{\partial x_k}\right)\frac{\varepsilon}{k}\overline{u_i'\phi'} + c_{\phi 2}\overline{u_j'\phi'}\frac{\partial u_i}{\partial x_j} + c_{\phi 3}\overline{u_j'\phi'}\frac{\partial u_j}{\partial x_i} + c_{\phi 4}\overline{u_i'u_j'}\frac{\partial \phi}{\partial x_j}\,. \tag{5}$$

emerge for the anisotropy tensor and the turbulent scalar flux vector, respectively. It is well known that strong curvature effects form a bottleneck for implicit and explicit algebraic models, also at the second order level modeling. Due to the inability of linear formulations for the pressure-stress relation, and the isotropic assumption for the turbulent dissipation tensor to well predict the main characteristics of the flow described above a nonlinear pressure-strain relation by Speziale et al. (1991), a curvature correction by Wallin and Johansson (see Gatski et al., 2004) and the anisotropy dissipation by Sjögren and Johansson (2000) have been considered. The resulting expression for the anisotropy tensor is:

$$a = \beta_1 S + \beta_2\left(S^2 - \frac{1}{3}II_s I\right) + \beta_3\left(\Omega^{*2} - \frac{1}{3}II_\Omega I\right) + \beta_4\left(S\Omega^* - \Omega^* S\right) + \beta_5\left(S^2\Omega^* - \Omega^* S^2\right) + \beta_6\left(S\Omega^{*2} - \Omega^{*2}S - \frac{2}{3}IVI\right) + \beta_7\left(S^2\Omega^{*2} + \Omega^{*2}S^2 - \frac{2}{3}VI\right) + \beta_8\left(S\Omega^* S^2 - S^2\Omega^* S^2\right) + \beta_9\left(\Omega^* S\Omega^{*2} - \Omega^{*2}S\Omega^*\right) + \beta_{10}\left(\Omega^* S^2\Omega^{*2} - \Omega^{*2}S^2\Omega^*\right), \tag{6}$$

where Ω^* is the curvature corrected vorticity tensor following Girimaji (1997), S the normalized symmetric part of the velocity gradient and

$$II_s = S^2 = S_{ij}S_{ij}\,,\ II_\Omega = \Omega^2 = \Omega_{ij}\Omega_{ji}$$
$$III = S^3 = S_{ij}S_{jk}S_{ki}\,,\ IV = S\Omega^2 = S_{ij}\Omega_{jk}\Omega\,, \tag{7}$$
$$V = S^2\Omega^2 = S_{ij}S_{jk}\Omega_{kj}\Omega_{jk}$$

are invariants. The anisotropy tensor is written in matrix form in (6). The detailed EARSM solution can been found in Wallin (2000). The unknown model coefficients, β, were determined following Sadiki et al. (2003) on the basis of Wallin (2000).

For the turbulent scalar flux it results:

$$-\rho\overline{u_i'\phi'} = -\left(1 - c_{\phi 4}\right)B_{ij}\frac{k}{\varepsilon}\overline{u_j'u_k'}\frac{\partial \bar{\phi}}{\partial x_k}\,, \tag{8}$$

where the tensor B_{ij} is an explicit function of the mean flow gradient normalized by turbulence time scale, the production to dissipation ratio, and the time scale ratio r:

$$B = \frac{\left(G^2 - \frac{1}{2}Q_1\right)I - G\left(c_s S + c_\Omega \Omega^*\right) + \left(c_s S_{ij} + c_\Omega \Omega^*\right)^2}{G^3 - \frac{1}{2}GQ_1 + \frac{1}{2}Q_2}\,, \tag{9}$$

where B is written in matrix form and I is the identity matrix. Moreover,

$$c_s = 1 - c_{\phi 2} - c_{\phi 3}, c_\Omega = 1 - c_{\phi 2} + c_{\phi 3}\,, \tag{10}$$

$$Q_1 = c_s^2 II_s + c_\Omega^2 II_\Omega\,;\ Q_2 = \frac{2}{3}c_s^3 III_s + 2c_s c_\Omega^2 IV\,. \tag{12}$$

Finally

$$G = \frac{1}{2}\left(2c_{\phi 1} - 1 - \frac{1}{r} - \frac{P}{\varepsilon}\right) \text{ with } r = \frac{k_\phi/\varepsilon_\phi}{k/\varepsilon} \approx 0.55\,. \tag{13}$$

All model coefficients are summarized in Tab. 1.

Table 1: Models coefficients.

A_1	A_2	A_3	A_4	$c_{\phi 1}$	$c_{\phi 2}$	$c_{\phi 3}$	$c_{\phi 4}$
1.2	0	1.8	2.25	4.46	-0.5	0.02	0.08

To account for the effects near the wall the Low-Re variant of EARSM is applied, where the anisotropy tensor is modified by the dump function along the line of Craft et al. (1996):

$$f_\mu = 1 - \exp\left[-\left(\mathrm{Re}_t/90\right)^{1/2} - \left(\mathrm{Re}_t/400\right)^2\right], \qquad (14)$$

where Re_t is the local Reynolds number. As reference model the Low-Re k-ε model of Chien (1982) is considered.

APPLICATIONS

The first configuration investigated here is known as ERCOFTAC-test case in the interest group "Refined turbulence modeling" to emphasize the joint effects of geometry confinement and swirling on turbulent flow and mixing. Experimentally investigated by Roback et. al. (1983) it is characterized by a small swirl number $S = 0.45$ (Fig. 1). The boundary conditions used correspond to the experimental data. The details of geometrical parameters are presented in Fig. 2, while all flow parameters are summarized in Tab. 2. In addition to the mean flow and turbulence fields, the experiment provided also the results for mean scalar (mixture fraction), scalar variance and scalar fluxes.

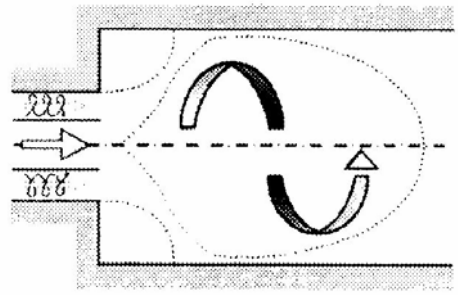

Figure 1: Swirled flow with small swirl number.

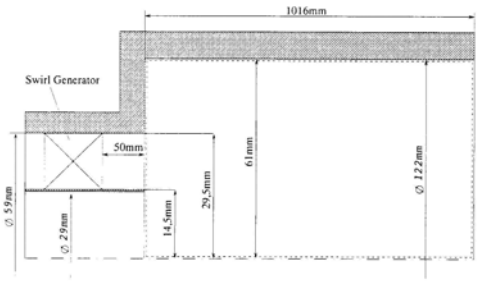

Figure 2: Description of combustor geometry ($S = 0.45$).

Table 2: Flow parameters.

	Primary inflow	Secondary (swirled) inflow
Re	15900	47500
Mean axial velocity (m/s)	0.66	1.52
Mass flow rate (kg/s)	0.391	3.331
Swirl number, S	0.0	0.45
Length scale	0.008	0.0045
Density (kg/m3)	1000	
Viscosity (Pas)	$9.84 \cdot 10^{-4}$	

The numerical grid used consisted of 80000 CV's. One of the most distinct features for this configuration is the formation of the central toroidal recirculation zone and the corner recirculation zone. Concerning the global flow pattern, both recirculation zones and reattachment point are better predicted with the models used (Fig. 3) than with the RSM by Jakirlic et al. ($x = 200$ mm) in comparison to experimental data (reattachment point of $x = 160$ mm measured).

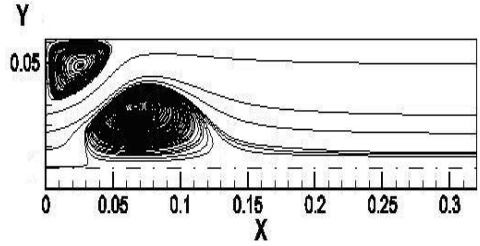

Figure 3: Streamlines in the combustor chamber with small swirl number.

In Fig. 4-6 three components of velocity achieved with $k-\varepsilon$ and EARSM are presented in comparison with experimental data. It can be seen that both models deliver good results for all components velocities after the reattachment point $x = 160$ mm. In recirculation zone ($x = 20...160$ mm), the EARSM appears to be more accurate than the $k-\varepsilon$ model. However the joint effects of the high expansion ratio ($ER = 2.1$) and swirling inflow contribute to the surprisingly good cut off of the standard $k-\varepsilon$ model after $x = 200$ mm. It must be mentioned that both the onset of the free separation zone and its length are correctly predicted by the advanced EARSM.

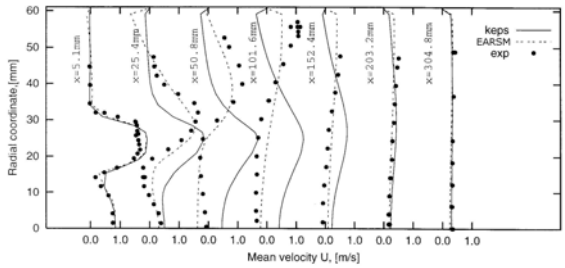

Figure 4: Mean axial velocity: comparison with experiment.

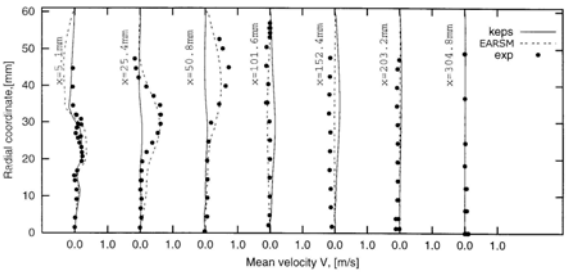

Figure 5: Mean radial velocity: comparison with experiment.

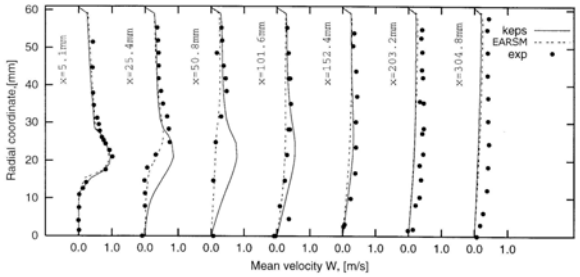

Figure 6: Mean tangential velocity: comparison with experiment.

The same prediction behavior can be observed for the kinetic energy (Fig. 7).

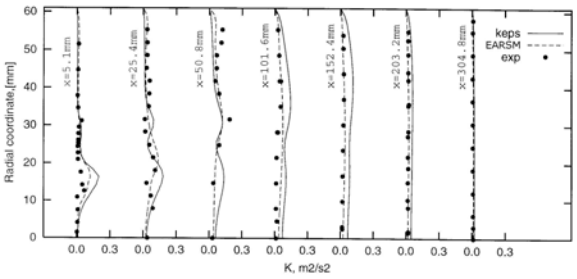

Figure 7: Turbulent kinetic energy: comparison with experiment.

With regard to the scalar field some results calculated by using the simple gradient model and the advanced EASFM for the mixing transport are displayed in Fig. 8-9 in comparison with experimental data.

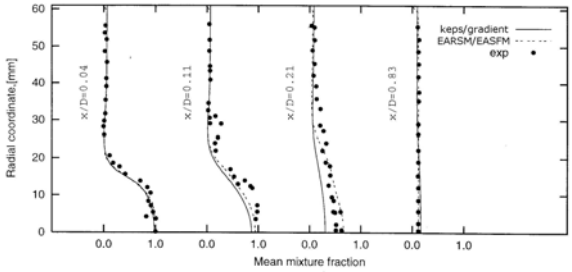

Figure 8: Mean mixture fraction: comparison with experiment.

The mean quantities are well predicted by both models as shown in Fig. 8. The change in profiles of mixture fraction indicates a rush spreading of the central stream i.e. very intensive mixing, which is completed already after three step heights ($x/D = 0.83$). Fig. 9 shows the evolution of the scalar flux obtained by using the advanced EARSM for the scalar transport model. The calculations with the advanced EARSM/EASFM result in a high negative value of the scalar flux in the outer part of the mixing layer, agreeing well with LES data (Pierce et al., 1998) and RSM (Jakirlic et al., 2004) in contrast to experiments. The results presented here however are better than that obtained using two dimensional RSM.

The second test case is the flow in U-duct channel. The geometry and numerical grids are shown in Fig. 10. This configuration was investigated experimentally by Chang et. al. (1983). Detailed measurements of the flow, temperature and Nusselt number by Johnson and Lauder (1985) made this U-bend an important and well-documented generic case for validation of numerical models for heat transfer applications.

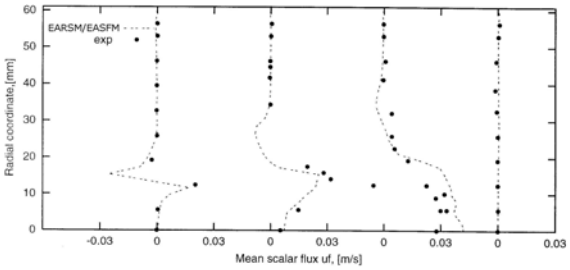

Figure 9: Mean scalar flux: comparison with experiment.

Johnson and Lauder used a $72D$ (*D:* the mean hydraulic diameter) long straight inlet and a $72D$ long straight outlet in order to achieve similar flow field as the one measured by Chang et. al. Constant wall heat flux was applied to the last $57D$ upstream the bend, the bend itself and the first $42D$ downstream the bend. The geometrical and fluid dynamic parameters are summarized in Table 3.

Table 3: Geometrical and fluid dynamic parameters.

D, mm	*U, m/s*	*Re*	R_c/D	*CV*
88.9	*8.93*	*56700*	*3.357*	*200000*

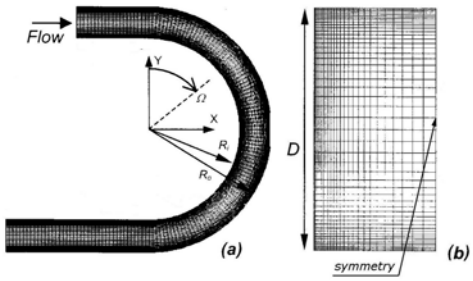

Figure. 10: Numerical setup of U-duct channel.

To get full developed turbulent flow before the turning, a square channel of $100D$ is used. To save computational time symmetry boundary conditions in the middle of channel are used (Fig. 10, b).
The grids were refined near the wall so that the first point is found at $y^+ = 1$. Prior numerical investigations of this configuration reported that models with wall function could not predict precisely the heat exchange on the wall. In the present work, an advanced model including a Low-Re formulation of EARSM/EASFM with curvature correction, anisotropy dissipation and nonlinear pressure strain rate is used for the velocity and temperature field, respectively.

In the following, results obtained with this model will be presented in comparison with the linear model and with experiments. In Fig. 11 the absolute velocity profiles are exhibited at different axial positions.

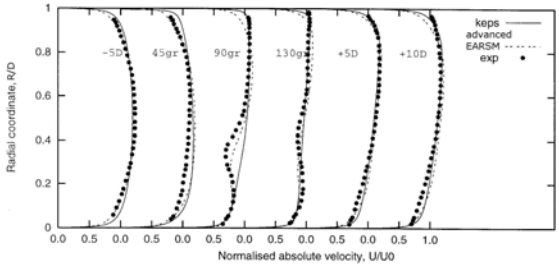

Figure 11: Mean absolute velocity on the symmetry plane.

Both models prediction achieves satisfactory agreement with experimental data, but the advanced model predicts accurately secondary streamlines effect in square channel that allows to get better results for U-duct also (see Fig. 12). It is worth mentioning that the center of the recirculation zone predicted lies at $y/H = 0.35$ where the pick is found in Fig. 13 and 14 for the (mean) velocity and temperature field, respectively.

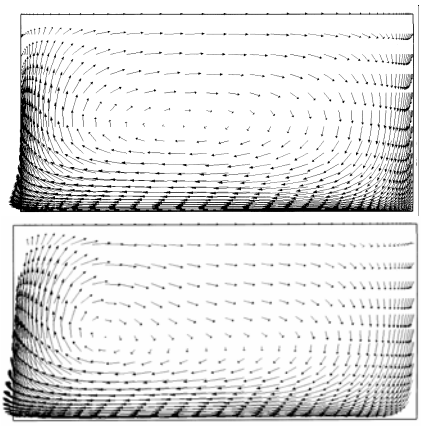

Figure 12: Secondary streamlines by $k-\varepsilon$ (above) and advanced EARSM (below).

This is obviously visible in section $\phi = 90°$. The velocity profile for this section is shown in Fig. 13. It can be seen clearly that the advanced EARSM predicts better the so called "camel effect".

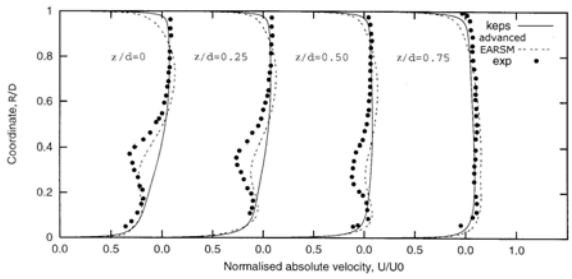

Figure 13: Mean absolute velocity in section $\phi = 90°$.

Regarding the scalar transport, the temperature profiles are shown at different axial positions in Fig. 14.

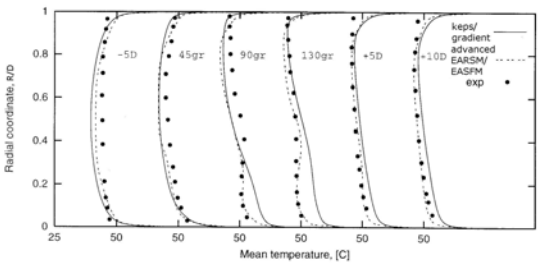

Figure 14: Mean temperature on the symmetry plane.

The same characteristics of the prediction behavior is observed for the advanced EASFM in comparison with the standard linear model.

Concerning the heat transfer prediction, the calculated local Nusselt numbers at the sections of $\phi = 0°$, $45°$, $90°$, $135°$, $180°$ are, respectively, compared with experimental data in Fig. 15. The levels of general agreement between the models and the experiments are fairly reasonable though some discrepancies can be found. In regions of the inner wall EASFM is obviously better. This is also the case right at the section $\phi = 0°$, 45° in all regions.

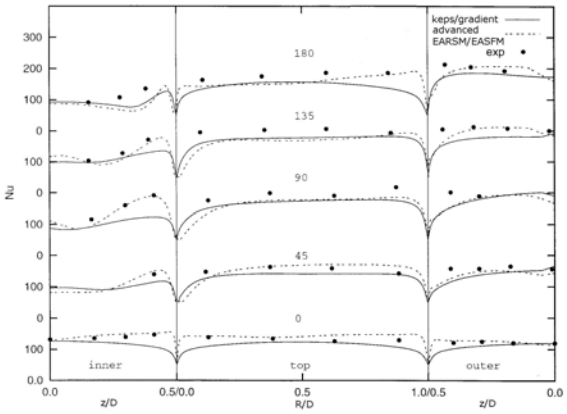

Figure 15: Local Nusselt number obtained using Low-Re $k-\varepsilon$ model and advanced EARSM.

CONCLUSION

To assess the advanced models used several aspects were investigated and following concluding remarks can be made:

1. The combination of advanced EARSM/EASFM allows to predict satisfactorily flow processes with mixing and heat transfer phenomena in complex configurations without numerical problems inherent to second order level-models.

2. In curved ducts of relevance in heat-exchangers, cooling passages of gas turbines and automobile engines, the existence of the so-called "camel back" shapes in the streamwise mean velocity and temperature distribution in the curvature has been predicted well, in contrast to linear, nonlinear $k-\varepsilon$ models and some models of second order level.

3. In swirled confined flows, turbulent flow and mixing processes dominated by the joint effects of geometry confinement (expansion ratio), circumferential velocity and swirl intensity (*S*) are satisfactorily described. Some results (turbulent scalar flux) are better than computations using second order level-models.

4. Dealing with configurations exhibiting strong wall effects, Low-Re approach is recommendable, as shown in this work. In such cases, LES can not be high performance. Therefore, the approach to get around the LES bottleneck tends remain the hybrid LES-RANS, in which RANS is used near wall while LES is utilized in the remaining part of the domain.

REFERENCES

Chang S.M., Humphrey J.A.C., Modavi A., 1983, Turbulent flow in a strongly curved U-Bend and downstream tangent of square cross-sections, Phys. Chem. Hydrodyn. 4 (3) 243-269.

Chien K., 1982, Predictions of Channel and Boundary-Layer Flows with a Low-Reynolds-Number Turbulence Model, AIAA, Vol. 20, pp. 33-38.

Craft T.J., Launder B.E. and Suga K., 1996, Development and application of a cubic eddy – viscosity model of turbulence, Int. J. Heat and Fluid Flow 17: 108-115.

Etemad S., Rokni M., Sunden B. and Daunis O., 2003, Analysis of Turbulent Flow and Heat Transfer in A Square-

Sectioned U-Bend, Turbulence Heat and mass Transfer 4. Begell House.

Gatski T.B., Wallin S., 2004, Extending the weak-equilibrium condition for algebraic Reynolds stress models to rotating and curved flows, JFM, vol. 518, pp. 147-155.

Girimaji S. S., 1997, A Galilean invariant explicit Reynolds stress model for turbulent curved flows. Phys. Fluids 9: 1067-1077.

Grundestam O., Wallin S., Johansson A., 2001, A generalized EARSM based on a nonlinear pressure strain rate model. Turbulence and Shear Flow Phenomena II, Stockholm, II: 223-228, June 27-29.

Jester-Zürker R., Jakirlic S., Tropea K., 2004, Computational modeling of turbulent mixing in confined swirling environment under constant and variable density conditions; flow, Turbulence and combustion, submitted.

Johnson R. W., Lauder B. E., 1985, Local Nusselt number and temperature field in turbulent flow through a heated square-sectioned U-bend, Int. J. Heat Fluid Flow 6, 171-180.

Leschziner, M.A., 2003, Modeling Separation from Curved Surfaces with anisotropy-resolving Turbulence Closures and related Supplementary Observations on LES, CHFF 03, Hungary.

Pierce C. D., Moin P., 1998, Large eddy simulation of a confined jet with swirl and heat release, AIAA, 98-2892.

Pope S.B., 2004, Ten questions concerning the large-eddy simulation of turbulent flows, New Journal of Physics (6).

Roback R., Johnson B.V., 1983, Mass and Momentum Turbulent Transport Experiments with Confined Swirling Coaxial jets, NASA Contractor Report 168252.

Sadiki A., Jakirlic S., Hanjalic K., 2003, Towards a Thermodynamically Consistent, Anisotropy-Resolving Turbulence Model for Conjugate Flow, Heat and Mass Transfer. Turbulence, Heat and Mass Transfer 4. Begell House.

Sjögren T. I., Johansson A. V., 2000, Development and calibration of algebraic non-linear models for terms in the Reynolds stress transport equations. Phys. Fluids 12: 1554-1572.

Speziale C.G., Sarkar S., Gatski T.B., 1991, Modeling the pressure strain correlation of turbulence: an invariant dynamical systems approach, J. Fluid Mech. 227:245-272.

Suga K., 2002, Predicting turbulence and heat transfer in 3-D curved ducts by near-wall second moment closures, International Journal of Heat and Mass Transfer 46.

Wallin S., 2000, Engineering turbulence modeling for CFD with a focus on explicit algebraic Reynolds stress models, Doctoral thesis, Norsteds Truckeri, Stockholm, Sweden.

Wikstrom P.M., Wallin S., Johansson A.V., 2000, Derivation and investigation of a new explicit algebraic model for the passive scalar flux, Phy. Fluids, 12:688-702.